Bioorg. Med. Chem. Lett. 49 (2021) 128308

Contents lists available at ScienceDirect

Bioorganic & Medicinal Chemistry Letters

journal homepage: www.elsevier.com/locate/bmcl

Induction of apoptosis, cytotoxicity and radiosensitization by novel 3,4-dihydroquinazolinone derivatives

Aiten M. Soliman [a], Amira Khalil [b], Eman Ramadan [c], Mostafa M. Ghorab [a,*]

[a] Department of Drug Radiation Research, National Center for Radiation Research and Technology (NCRRT), Egyptian Atomic Energy Authority (EAEA), Cairo 11765, Egypt
[b] The Center for Drug Research and Development (CDRD), Pharmaceutical Chemistry Department, Faculty of Pharmacy, The British University in Egypt (BUE), El-Sherouk City, Cairo 11837, Egypt
[c] Pharmacology and Biochemistry Department, Faculty of Pharmacy, The British University in Egypt (BUE), El-Sherouk City, Cairo 11837, Egypt

ARTICLE INFO

Keywords:
3,4-Dihydroquinazolinone
Sulfonamide
Apoptosis
EGFR
XIAP
Docking

ABSTRACT

Twenty new quinazolinone derivatives bearing a piperonyl moiety were designed and synthesized. The structures of the target compounds were in agreement with the microanalytical and spectral data. Compounds **4-10, 13, 14** and **17-27** were screened for their cytotoxic activity against HepG-2 and MCF-7 cancer cell lines. The target compounds showed IC_{50} in the range of 2.46–36.85 μM and 3.87–88.93 μM for HepG-2 and MCF-7, respectively. The promising compounds **7, 19, 26** and **27** were selected to measure their EGFR inhibitory activity. The IC_{50} values of the promising compounds were in the range of 146.9–1032.7 nM for EGFR in reference to Erlotinib (IC_{50} = 96.6 nM). In further studies on compounds **7, 19, 26** and **27** using HepG-2 cell line, there was significant overexpression of p21 and downregulation of two members of IAPs protein family; Survivin and XIAP, relative to their controls. Annexin V-FITC and caspase-3 analyses have established a significant increase in early apoptosis. Moreover, the four selected compounds have impaired cell proliferation by cell cycle arrest at the G2/M phase compared to their respective control. Considering radiotherapy as the primary treatment for many types of solid tumors, the radiosensitizing abilities of compounds **7, 19, 26** and **27** were measured against HepG-2 and MCF-7 cell lines combined with a single dose of 8 Gy gamma radiation. Measurement of the IC_{50} of the promising compounds after irradiation revealed their ability to sensitize the cells to the lethal effect of gamma irradiation (IC_{50} = 1.56–4.32 μM and 3.06–5.93 μM for HepG-2 and MCF-7 cells, respectively). Molecular docking was performed to gain insights into the ligand-binding interactions of **7, 19, 26** and **27** inside the EGFR binding sites and revealed their essential interactions, explaining their good activity towards EGFR.

Cancer initiation and progression are due to several external environmental risk factors combined with internal genetic mutations.[1] Despite the presence of various types of cancer treatments, limitations in current therapies exist as chemo-resistance,[2] relapses and toxic effects. This occurs due to poor selectivity resulting in off-target side effects that seriously affect the patient's quality of life.[3] Targeted chemotherapies usually aim at the tumor microenvironment, regulate the tumor cell cycle and induce apoptosis.[4]

Apoptosis is a genetically programmed mechanism critical for the survival and normal functioning of the cells.[5] Cancer is characterized by suppression of the apoptotic mechanisms resulting in treatment resistance.[6] Among the essential regulators of apoptosis is a family of enzymes known as caspases that play a significant role in balancing cellular inflammation and death.[7] During tumor progression, there is an accumulation of various inhibitors of apoptosis proteins (IAPs) within the cells.[8] IAP family of proteins could inhibit the enzymatic activity of caspases. Different IAPs, including XIAP, c-IAP1, c-IAP2 and Survivin, were identified to inhibit initiator caspase-9 and effector caspases 3 and 7.[9] Both XIAP and Survivin expression have been linked to both tumor recurrence and poor prognosis.

Moreover, apoptosis is triggered by selective crosslinking and inhibition of receptor tyrosine kinases (RTKs).[10] TKs are considered the most prevalent therapeutic targets in anticancer drug development.[11] The epidermal growth factor receptor (EGFR) belongs to protein tyrosine kinases and plays a critical role in cellular proliferation, differentiation and survival of normal as well as cancer cells.[12,13] Overexpression of

* Corresponding author.
E-mail address: mmsghorab@yahoo.com (M.M. Ghorab).

https://doi.org/10.1016/j.bmcl.2021.128308
Received 21 May 2021; Received in revised form 27 July 2021; Accepted 31 July 2021
Available online 4 August 2021

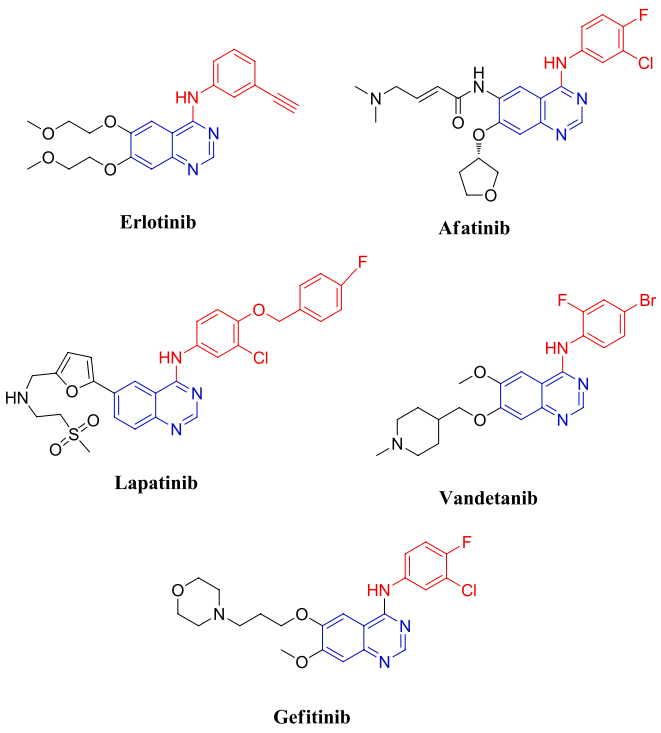

Fig. 1. Chemical structures of FDA-approved TK inhibitors showing quinazoline scaffold.

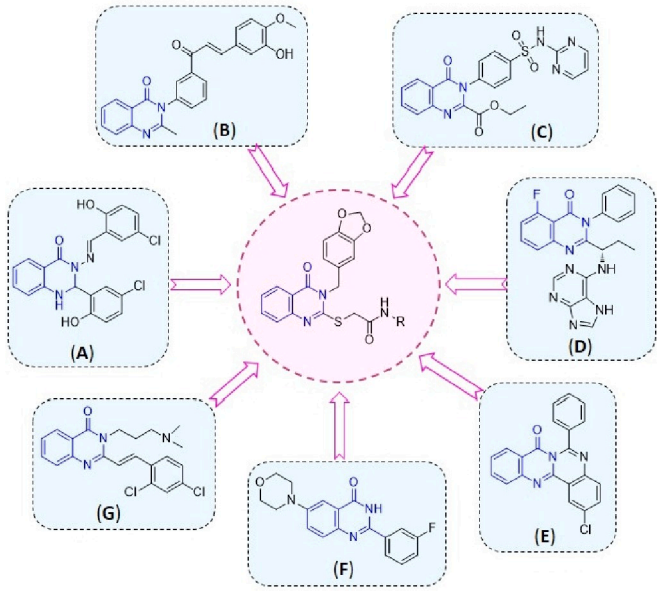

Fig. 2. The design strategy of our target compounds.

EGFR is evident in different types of tumors such as breast, ovarian and squamous cell cancers, [14] leading to irregular apoptosis and uncontrolled cellular proliferation.[15] Seeking EGFR inhibition using small molecules novel agents has been an interesting and promising area for selective cancer treatment.

Quinazoline is an attractive chemical scaffold displaying a wide spectrum of biological activities. [16–20] In our previous work, we have paid great interest in investigating quinazolines as anticancer agents.[21–23] Quinazoline as a chemical scaffold is a common pharmacophore among many reported EGFR inhibitors. [24] Fig. 1 shows examples of FDA-approved quinazolines that acts as multi-target TK inhibitors, mostly EGFR inhibitors as; Erlotinib, Afatinib, Lapatinib, Vandetanib and Gefitinib.[25]

Similarly, Sulfonamide moiety represents the core of many clinically used drugs comprising different pharmacological activities, including anticancer activity. [26] They exert their anticancer effect through a variety of mechanisms, mainly by carbonic anhydrase inhibition.[27,28] Furthermore, compounds having piperonyl ring exhibited a wide range of biological activities. They act as a potential pharmacophore with various activities as COX-2 inhibitors,[29] antiviral, [30] anticancer, [31] and apoptosis inducers.[32]

In this current work, we designed our library based on many representative quinazolinones possessing interesting anticancer and apoptotic inducer activity (Fig. 2) as follows; the 3-((5-chloro-2-hydroxybenzylidene)amino)-2-(5-chloro-2-hydroxyphenyl)-2,3-dihydroquinazolin-4(*1H*)-one (**A**) reported by Zahedifard and co-workers was found to cause significant inhibition on MCF-7 and MDA-MB-231 cell viability and to induce extrinsic and intrinsic apoptosis pathways by cytochrome *C* activated caspase-9 expression.[33] Wani *et al.* synthesized the quinazolinone chalcone (**B**), that induced mitochondrial dependent apoptosis, inhibited PI3K/Akt/mTOR signaling pathway in human colon cancer cells and arrested the cell cycle at the S and G2/M phases of the HCT-116 cells.[34] Nowar and her colleagues reported the quinazolinone-benzenesulfonamide derivative (**C**) to act as an antiproliferative and apoptosis inducer through the activation of caspases 3, 8 and 9 in HCT-116 cell line.[35] Idelalisib (**D**), an FDA-approved selective PI3Kδ inhibitor used for lymphoma treatment, can promote Bim-dependent apoptosis in hepatocellular carcinoma.[36] The natural 2-chloro-6-phenyl-8*H*-quinazolino[4,3-*b*]quinazolin-8-one (**E**) isolated from marine sponge, deemed to induce apoptosis in breast cancer cells via ROS production.[37] Moreover, the 2-(3-fluorophenyl)-6-morpholinoquinazolin-4(*3H*)-one (**F**) induced cell cycle arrest at the G2/M phase. It can be combined with 5-fluorouracil (5-FU) to cause a synergistic toxic effect on oral squamous cell carcinoma (OSCC).[38] Also, the (*E*)-2-(2,4-dichlorostyryl)-3-(3-(dimethylamino)propyl) quinazolin-4(*3H*)-one (**G**) synthesized by Zhang *et al.*[39] exerted its anticancer effect by arresting the mutant p53 function to trigger the deregulation of Cdk2 caused Bim-mediated apoptosis.

In this article, the target compounds were designed based on an interesting hybrid drug approach to have a quinazoline ring as the main building block. We also wanted to explore the effect of incorporating piperonyl group and sulfonamide moiety in the designed compounds. We will explore the chemical synthesis of the novel 3, 4 dihydroquinazoline piperonyl derivatives and their cytotoxic effect against breast cancer (MCF-7) as well as hepatic cancer (HepG-2) cell lines and their enzymatic inhibitory activity against the EGFR. Also, to study the potential effects of the promising compounds on cell cycle, caspases, XIAP and their use as promising apoptosis inducers. Furthermore, molecular docking was carried out inside the active site of EGFR to determine the possible binding interactions between the promising compounds and the receptor.

Schemes 1-3 show our synthetic strategy for preparing the desired quinazoline derivatives **4-10, 13, 14** and **17-27**. The methyl 2-aminobenzoate **1** was reacted with thiophosgene to yield the isothiocyanatobenzoate derivative **2**,[40] which was further reacted with piperonylamine **3** in dimethylformamide (DMF) and few drops of triethylamine (TEA) to yield our starting material the 3-(benzo[d][1,3]dioxol-5-ylmethyl)-2-mercaptoquinazolin-4(3*H*)-one **4**. The synthesis of a key hydrazide compound **6** was illustrated in Scheme 1 and proceeded by the reflux of compound **4** with ethyl bromoacetate in acetone containing K_2CO_3 forming the acetate derivative **5**. A solution of compound **5** was refluxed in ethanol containing hydrazine hydrate to produce our target hydrazide compound **6** in a decent yield. ^{1}H NMR of **6** confirmed the disappearance of the ethyl protons of compound **5** and the appearance of NH_2 protons of **6** (see experimental section).

The hydrazide compound **6** was used for the synthesis of compounds **7–10, 13, 14, 17** and **18** according to Schemes 1 & 2. Nucleophilic

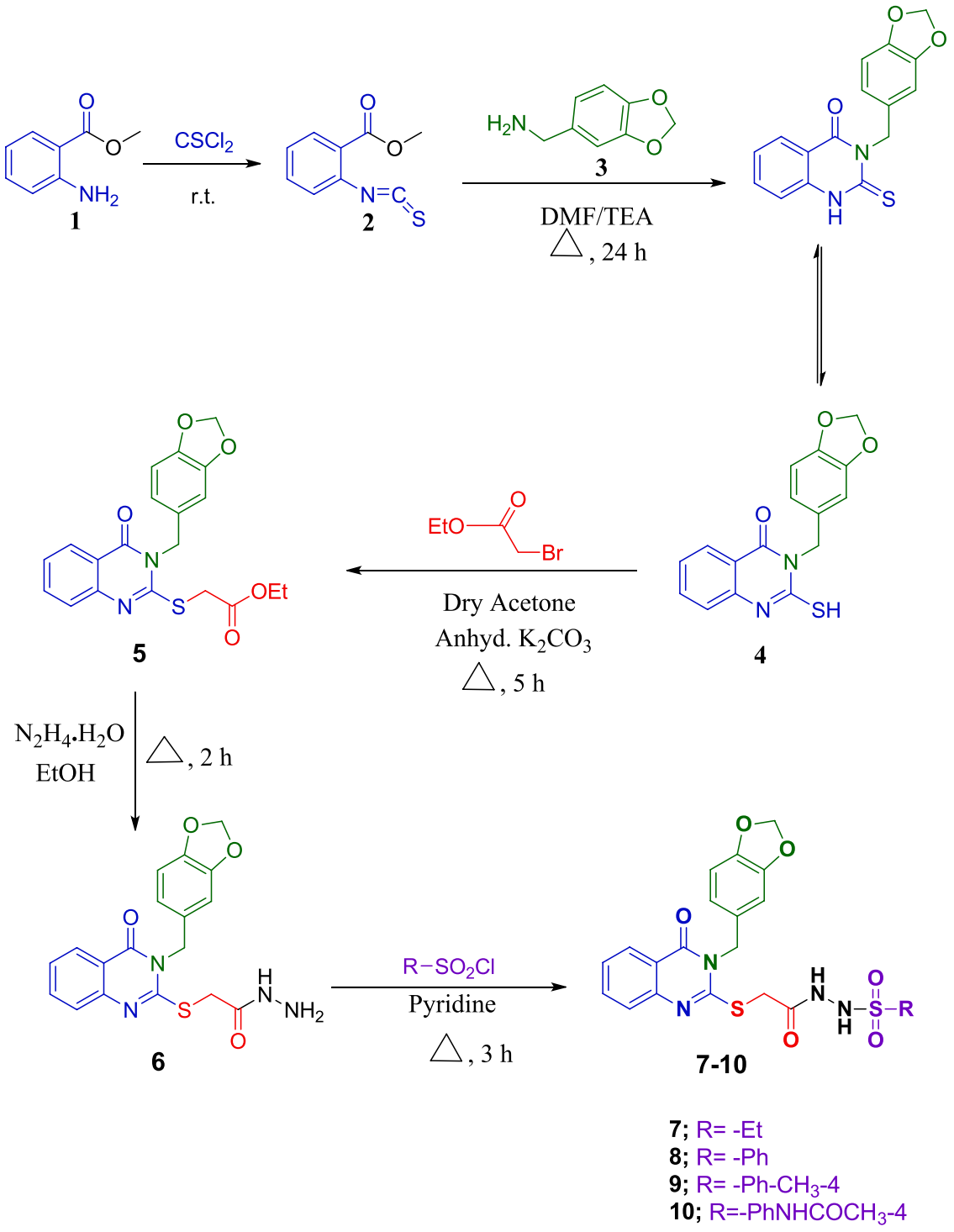

Scheme 1. Synthesis of compounds **4**-**10**.

reaction between compound **6** and different sulfonyl chloride derivatives in the presence of pyridine afforded **7**–**10** in good yield in the range of 72–80 %. The ^{1}H NMR spectrum of compound **7** showed characteristic triplet and quartet at 1.21 and 4.13 ppm due to the ethyl group, which corresponds to 14.61 and 61.57 ppm in ^{13}C NMR. A representative singlet appeared in the ^{1}H NMR of **9** at 2.26 ppm attributed to the CH_3 hydrogens and corresponds to 21.44 pm at ^{13}C NMR. Also, the acetamide group of **10** was peculiar in the NMR spectra.

Furthermore, compound **6** was allowed to react with acetophenone derivatives **11** and **12** in the presence of ethanol and glacial acetic acid under reflux. The resulted candidates **13** and **14** were produced in good yield, Scheme 2. Structure elucidation for **13** and **14** was confirmed mainly through H^{1}-NMR. The proton NMR spectrum for **13** revealed the obvious ethyl protons, whereas compound **14**′s spectrum showed a singlet peak for $COCH_3$ protons at 2.05 ppm. The hydrazinecarbothioamide derivatives **17** and **18** were produced by the reaction of the hydrazide **6** and the corresponding isothiocyanate benzenesulfonamide derivatives **15** and **16** in pyridine under reflux conditions as illustrated in Scheme 2. The open-chain derivatives were believed to be formed through nucleophilic substitution.

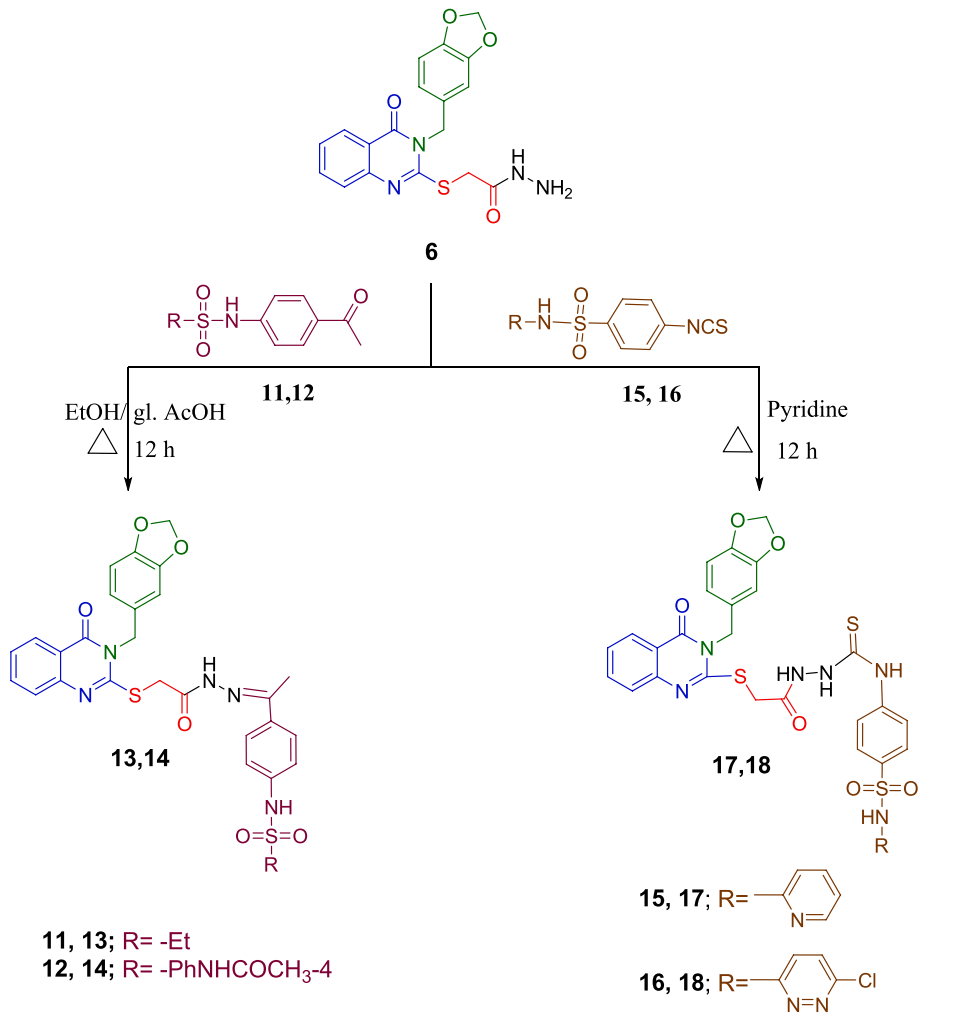

Scheme 2. Synthesis of compounds **13, 14, 17** and **18.**

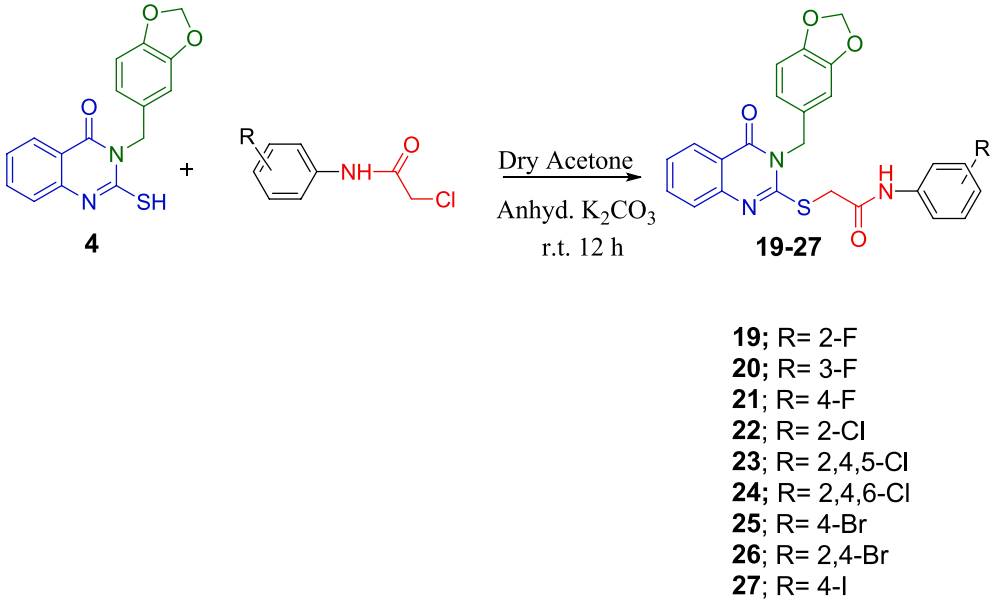

Scheme 3. Synthesis of compounds **19–27.**

Table 1
The IC_{50} values (μM) of compounds **4-10**, **13**, **14**, **17-27** against HepG-2 and MCF-7 cell lines using MTT assay.

Compound no.	HepG-2 IC_{50} (μM)*	MCF-7 IC_{50} (μM)*
4	27.26 ± 0.31	26.64 ± 0.42
5	–	–
6	8.15 ± 0.17	20.69 ± 0.35
7	8.76 ± 0.20	15.32 ± 0.33
8	22.20 ± 0.31	88.93 ± 4.01
9	28.16 ± 0.20	49.77 ± 0.14
10	33.94 ± 0.28	11.41 ± 0.32
13	9.08 ± 0.13	13.92 ± 0.25
14	4.21 ± 0.17	15.10 ± 0.13
17	36.85 ± 0.25	3.87 ± 0.10
18	9.34 ± 0.34	46.03 ± 0.08
19	2.46 ± 0.27	5.86 ± 0.184
20	8.51 ± 0.33	7.60 ± 0.31
21	7.18 ± 0.21	14.54 ± 0.33
22	17.87 ± 0.10	10.33 ± 0.49
23	12.09 ± 0.26	26.12 ± 0.56
24	–	–
25	11.13 ± 0.15	20.36 ± 0.33
26	4.01 ± 0.14	14.93 ± 0.23
27	13.17 ± 0.36	6.84 ± 0.15
Doxorubicin	8.90 ± 0.39	9.34 ± 0.24
Erlotinib	10.17 ± 0.32	12.40 ± 0.37

*The values represent the mean ± SD of three independent experiments.

Table 2
EGFR inhibitory activities of compounds **7, 19, 26** and **27** compared to Erlotinib (IC_{50}, nM).

Compound no.	IC_{50} (nM)[a]
7	146.9 ± 3.6
19	207.1 ± 4.9
26	1032.7 ± 31.8
27	754.3 ± 22.0
Erlotinib	96.6 ± 2.0

[a] The values represent the mean of three independent experiments ± SD.

The synthesis of compounds **19**–**27** was performed by the reaction of compound **4** [41] with the corresponding series of *N*-chloro substituted acetamides in acetone containing K_2CO_3 to produce a series of halogenated quinazolinone derivatives **19**–**27** in excellent yield. These hybrid molecules were synthesized by introducing halogenated phenyl groups on the acetamide tail to provide a set of compounds having variable lipophilic and electronic nature to study the structure–activity relationship (SAR). The structures of the target compounds were confirmed by spectroscopic data. IR spectra of **19**–**27** showed NH groups and 2CO bands at their identified region. ^{1}H NMR spectra revealed two singlets attributed to the S-CH_2 and NH protons. ^{13}C NMR spectra exhibited an up-field signal for the S-CH_2 and two downfield signals for the 2CO carbons.

The potential cytotoxic effect of the synthesized quinazolinone **4-10**, **13**, **14** and **17-27** on the viability of HepG-2 and MCF-7 were detected by MTT assay. The cell viability is expressed as percent of viable cells (mean ± SD) compared to untreated cells (taken as 100 % viable) for 24 hr by serial dilution. The estimated IC_{50} value (concentration that inhibits growth by 50%) of the target compounds against HepG-2 and MCF-7 cell lines are listed in Table 1. The initial cytotoxicity screening showed that compounds **4, 6-10**, **13**, **14**, **17-23** and **25-27** were effective against both HepG-2 cells and MCF-7 cells except for compounds **5** and **24** due to irregular concentration–response relationship. Table 1 shows that compounds **4, 6-10**, **13**, **14**, **17-23** and **25-27** have significant cytotoxic effects on HepG-2 and MCF-7 with IC_{50} values in the range of 2.46–36.85 μM and 3.87–88.93 μM, respectively. Doxorubicin and

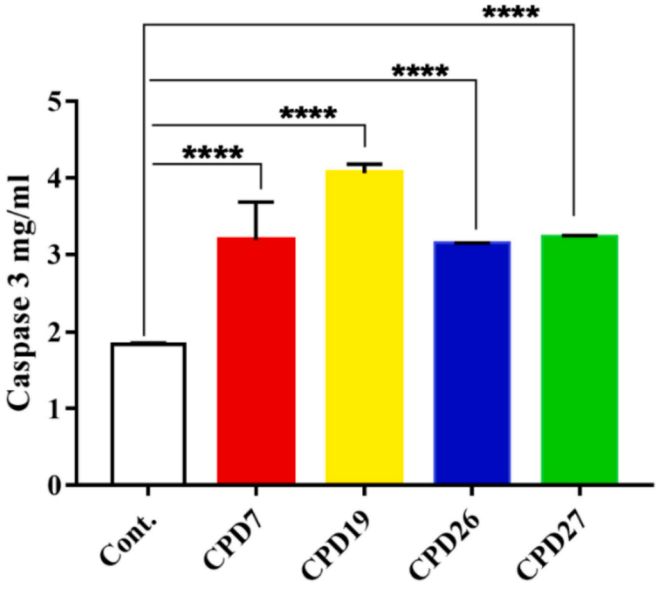

Fig. 4. Effect of compounds **7, 19, 26** & **27** on the secretion of caspase-3 in HepG-2 cells. The level of caspase-3 in cultural medium was assessed by ELISA showing significant increase compared to untreated control. Values are presented as means ± SD, ****, <0.0001, Vs respective control (n = 3).

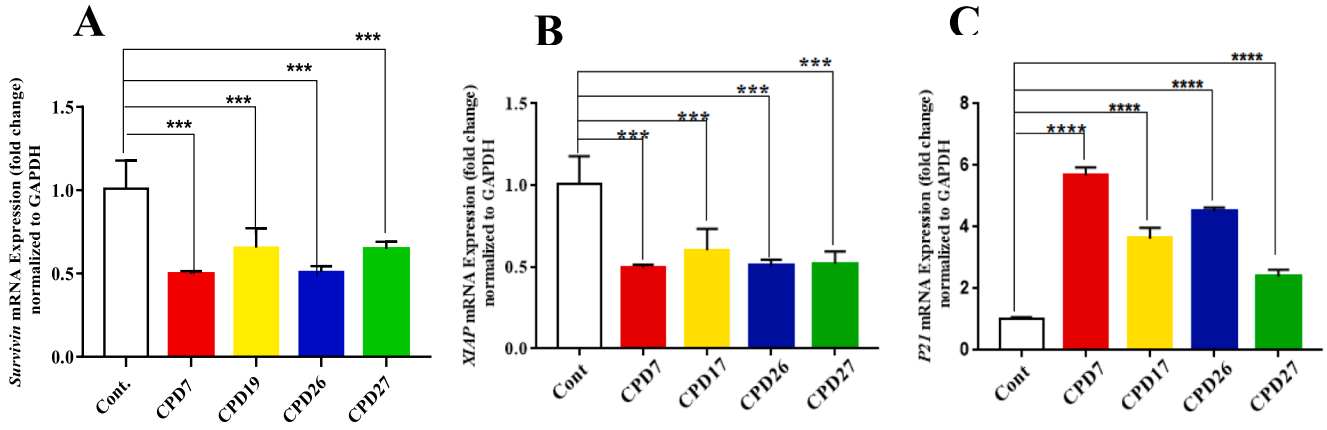

Fig. 3. Effect of compounds **7, 19, 26** & **27** on transcriptional level of Survivin (A), XIAP (B) and p21 (C). The relative mRNA expression of each gene was measured using real-time RT-PCR on HepG-2 cells treated with compounds **7, 19, 26** & **27** after normalizing the cycle thresholds (Ct) of each triplicate against their corresponding GAPDH. Data are expressed as mean ± S.E. ***, <0.0005, ****, <0.0001, Vs respective control (n = 3).

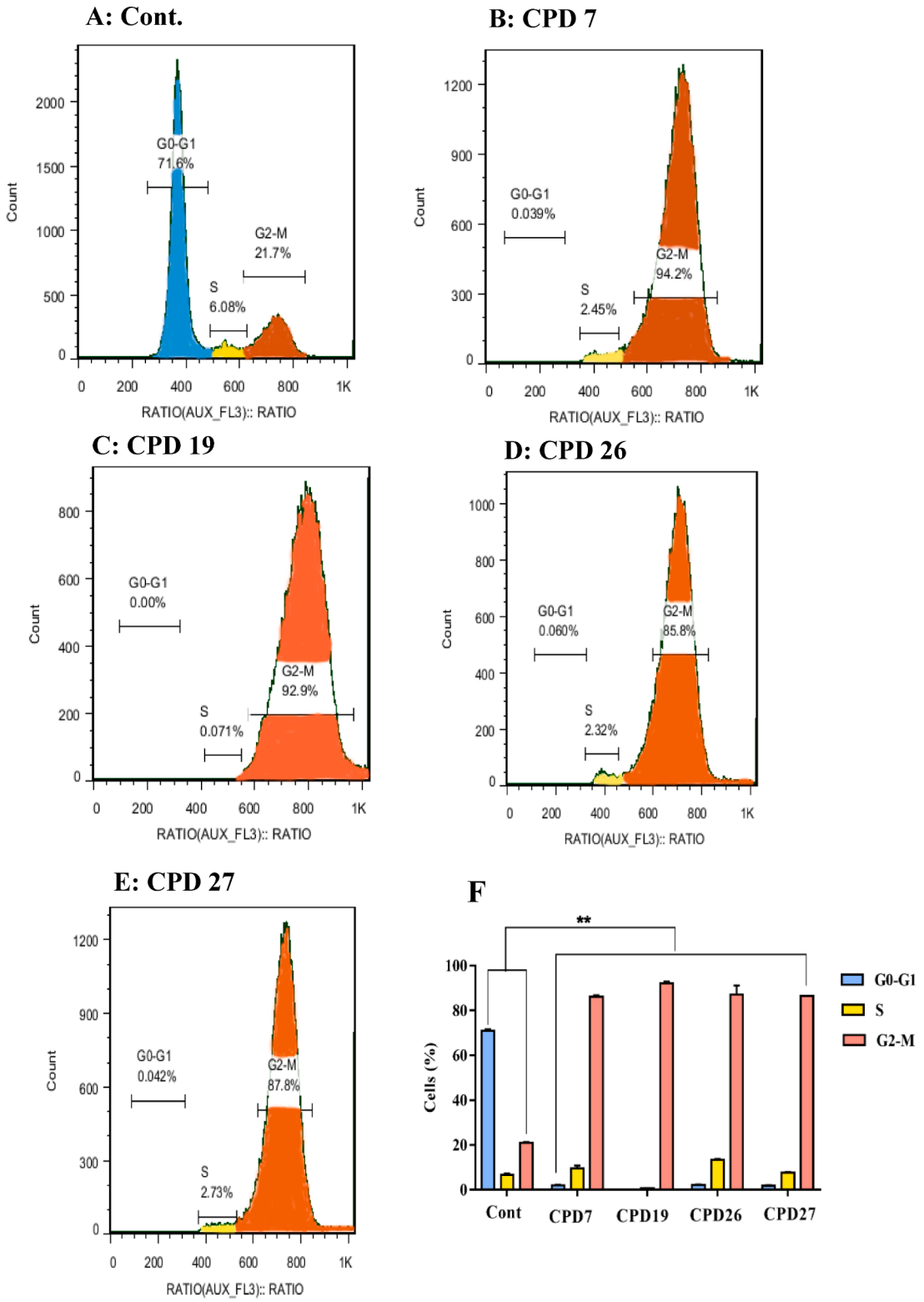

Fig. 5. Effect of compounds **7, 19, 26** & **27** on cell cycle distribution. Treatment of HepG-2 cells by compounds **7, 19, 26** & **27** have significantly increased the proportion of G2/M phase while significant decrease of G1-G0 and S phases compared to control. A) DMSO treated HepG-2 cells used as control. B) Treated HepG-2 with **7**. C) Treated HepG-2 with **19**. D) Treated HepG-2 with **26**. E) Treated HepG-2 with **27**. E) Percentage of cell populations. Values are presented as means ± SD, **, $p < 0.0022$ Vs respective control (n = 3).

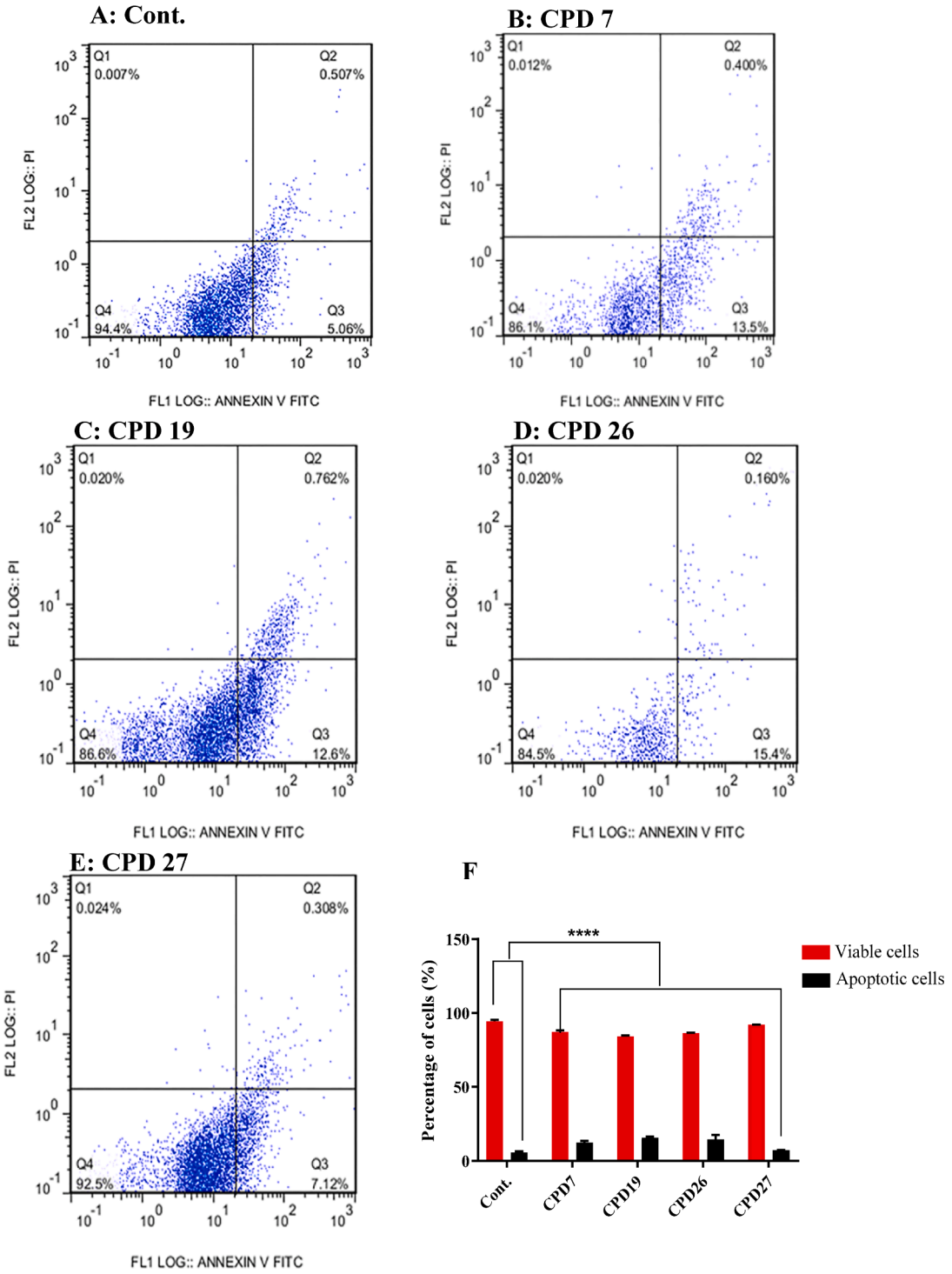

Fig. 6. Annexin V-FITC/PI double staining analysis of apoptosis in compounds **7, 19, 26** & **27** treated HepG-2 cells (A) HepG-2 control cells (B) HepG-2 cells treated with **7**C) HepG-2 cells with **19** (D) HepG-2 cells with **26.** (E) HepG-2 cells with **27**. Top right quadrant, dead cells in a late stage of apoptosis (Q2); bottom right quadrant (Q3), cells are undergoing apoptosis; bottom left quadrant, viable cells (Q1). (E): Chart comparison of cell distribution after treatment with compounds **7, 19, 26** & **27**. Values are presented as means ± SD, with significant, **** $p < 0.000$ Vs. respective control (n = 3).

Erlotinib were used as reference drugs, with IC_{50} 8.90, 10.17 μM for HepG-2 cells and 9.34, 12.40 μM for MCF-7 cells, respectively. The 2-((3-(benzo[d][1,3]dioxol-5-ylmethyl)-4-oxo-3,4-dihydroquinazolin-2-yl) thio)-*N*-(2-fluorophenyl)acetamide **19** has shown a potent cytotoxic effect on both HepG-2 and MCF-7 with IC_{50} values of 2.46 and 5.86 μM, respectively. It was also observed that the acetamide derivatives bearing halogens **19**–**27** showed very promising activity on HepG-2 cells in the range of 2.46–17.87 μM and 5.86–26.12 μM for MCF-7 cells except for compound **24**. Based on our results, we choose to conduct further investigation on the quinazolinone sulfonamide derivative **7** and the quinazolinone derivatives **19, 26** & **27** displaying promising cytotoxicity on both cell lines. The HepG-2 cells were chosen to conduct the apoptosis and cell cycle analysis tests as the compounds showed significant cytotoxicity compared to the MCF-7 cells. IC_{50} values of the

Table 3
The cytotoxicity of the promising compounds **7, 19, 26** and **27** after irradiation.

Compound no.	HepG-2 C_{50} (μM)[b]	MCF-7 IC_{50} (μM)[b]
7	2.25 ± 0.04	5.93 ± 0.16
19	1.56 ± 0.05	3.06 ± 0.02
26	1.76 ± 0.07	4.91 ± 0.21
27	4.32 ± 0.23	4.69 ± 0.32

[b] Represents the mean of three independent experiments ± SD.

most potent compounds are in the range of 2.46–13.17 μM for HepG-2 cell line.

The promising compounds **7, 19, 26** and **27** were subjected to EGFR-TK inhibitory assay compared to Erlotinib. Table 2 demonstrated the inhibition values of these compounds against EGFR. The IC_{50} values were in the range of 146.9–1032.7 nM versus 96.6 nM for Erlotinib. Regarding the *N'*-(2-((3-(benzo[d][1,3]dioxol-5-ylmethyl)-4-oxo-3,4-dihydroquinazolin-2-yl)thio)acetyl)ethanesulfonohydrazide **7** was found to be the most potent in this study. The 2-((3-(benzo[d][1,3]dioxol-5-ylmethyl)-4-oxo-3,4-dihydroquinazolin-2-yl)thio)-*N*-(2-fluorophenyl)acetamide **19** displaying the most potent cytotoxic activity towards the HepG-2 cells comes in the second place in EGFR inhibitory activity (IC_{50} = 207.1 nM). The promising candidates were further subjected to cell cycle analysis and apoptotic assay.

Inhibitors of apoptosis proteins (IAP) are a family of proteins that inhibit apoptosis induced by several pro-apoptotic stimuli.[42] The IAP family includes XIAP and Survivin; their expression has been linked to poor prognosis, increased tumor recurrence and radioresistance in many

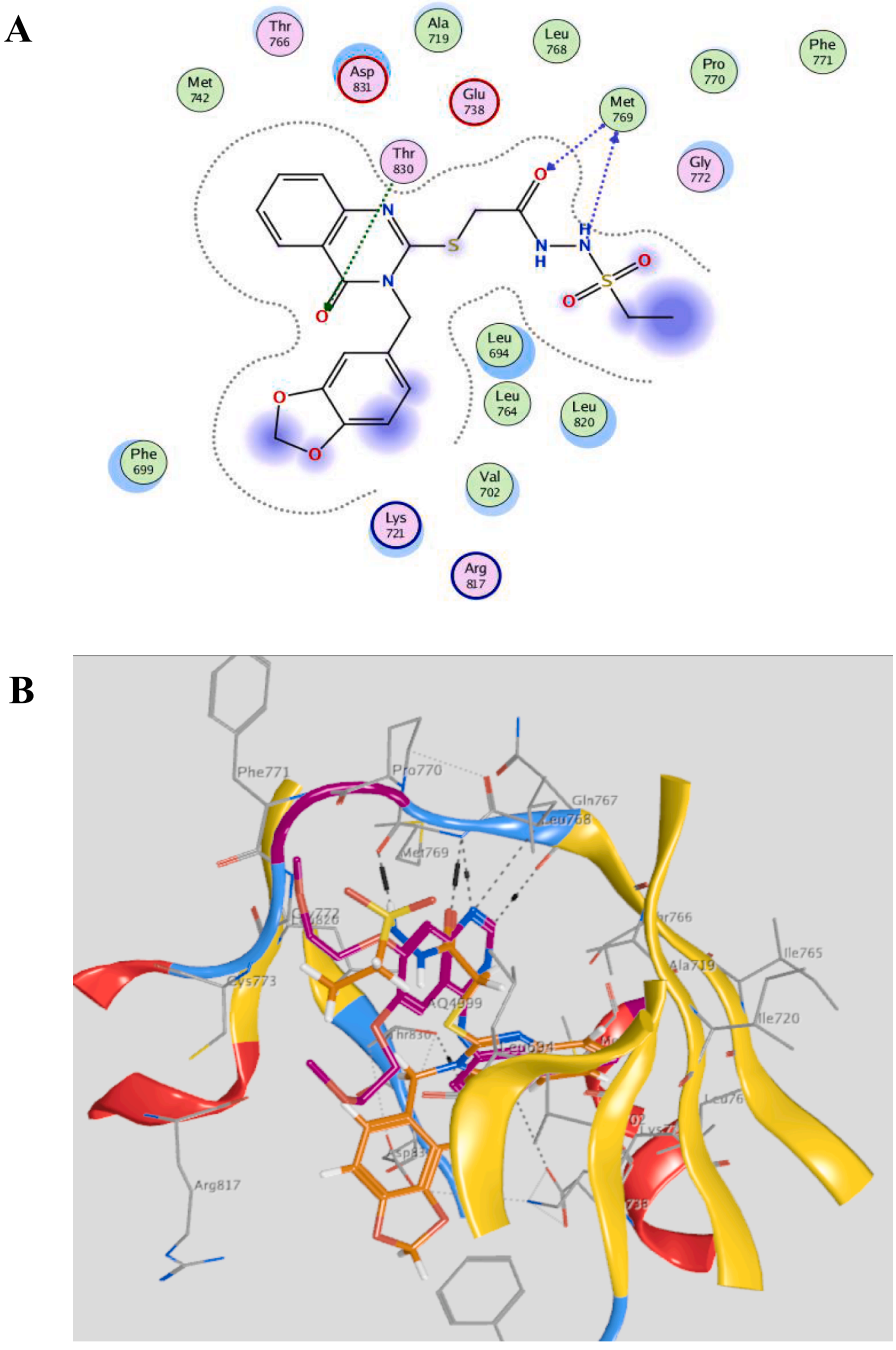

Fig. 7. A: 2D docking pose of compound **7**, **B:** 3D interactions of **7** (brown), superimposed on the native ligand erlotinib (magenta).

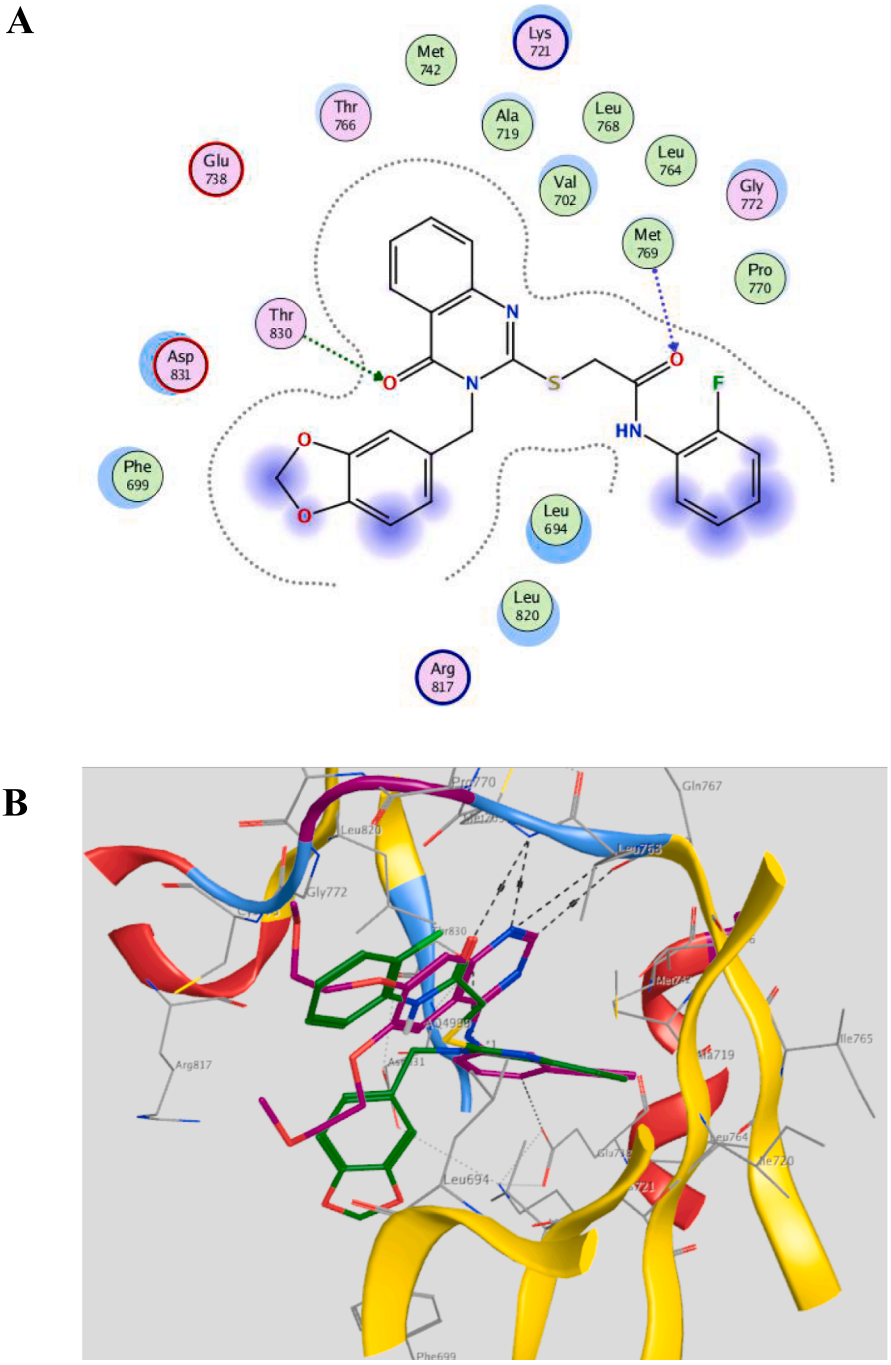

Fig. 8. A: 2D interaction map of compound **19, B:** 3D interaction pose of **19** (green), superimposed on the native ligand erlotinib (magenta).

cancer types.[43] Accordingly, blocking of Survivin and XIAP expression is becoming a promising strategy in cancer therapy.[44] HepG-2 cells were treated with compounds **7, 19, 26** & **27** to measure relative mRNA expression of Survivin, XIAP and p21 mRNA using real-time RT-PCR after normalizing the cycle thresholds (Ct) of each triplicate against their corresponding control GAPDH. In this study, treatment of HepG-2 cells with the selected compounds has decreased the relative mRNA expression of XIAP and Survivin by almost 50% compared to control (Fig. 3**A and 3B**).

Moreover, many studies have proven that increased expression of IAP proteins, especially XIAP and Survivin are associated with radioresistance.[43] Our data show significant downregulation of XIAP and Survivin expression in HepG-2 treated cells relative to untreated control, suggesting that these novel quinazolinones could be a potent radiosensitizing agent for hepatocellular carcinoma.

P21 has a well-described molecular role in carcinogenesis of tumors, not only in proliferation arrest but also during apoptosis.[45] Compounds **7, 19, 26** & **27** treatment of HepG-2 have upregulated the cyclin-dependent kinase inhibitor p21 mRNA expression (~500%, 400%, 400% and 200%, respectively) in comparison to control (Fig. 3**C**). P21 is a key cell cycle regulator that plays an important role in growth inhibition and overexpression leads to G_1, G_2, or S-phase arrest.[46] Our cell cycle analysis data have shown significant G2/M arrest which may be related to p21 overexpression (Fig. 3**C,** Fig. 5). Taken together, these results suggest that **7, 19, 26** & **27** treatment is responsible for overcoming apoptosis resistance and arresting the proliferation of HepG-2 by

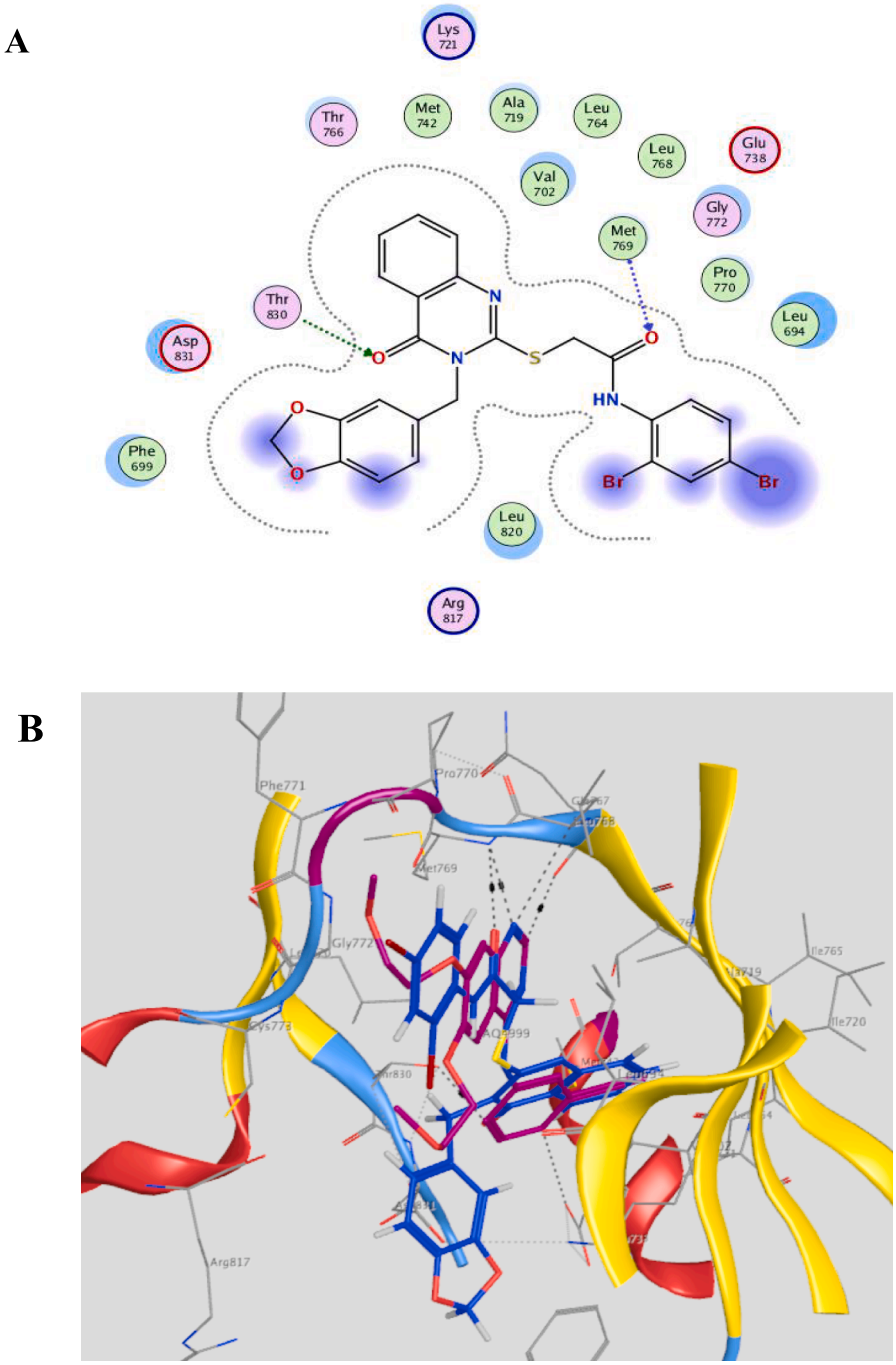

Fig. 9. A: 2D docking pose of compound **26**, B: **3D** interactions of **26** (blue), superimposed on the native ligand erlotinib (magenta).

suppressing Survivin and XIAP and overexpressing p21 (Fig. 3).

Active caspase-3 is a critical executioner of apoptosis. It is an inactive proenzyme activated by extrinsic (death ligand) and intrinsic (mitochondrial) pathways leading to cell death.[47] In many types of cancer, the over-expressed IAPs interact with caspase-9 preventing the activation of caspase-3.[48] So IAPs employ their antiapoptotic activity through direct inhibition of active caspases.[49] HepG-2 cells were treated with compounds **7, 19, 26** & **27** and caspase-3 level was evaluated using ELISA Kit. The compounds have decreased the relative mRNA expression of XIAP and Survivin by almost 50% compared to control (Fig. 3**A and 3B**). As expected, on evaluation of caspase-3 level of treated HepG-2 with the promising compounds, caspase-3 level has increased approximately 50% (for compounds **7, 26** and **27**) and 100% (for compound **19**) in comparison to DMSO treated HepG-2 cells used as control (Fig. 4). Our data suggests that the decreased level of caspase-3 is due to decreased expression of XIAP and Survivin upon treatment of HepG-2 by the selected compounds.

Progression of eukaryotic cells through the cell cycle is controlled by successive stimulation and inhibition by cyclin-dependent kinases (CDKs) and associated cyclin subunits at specific checkpoints to ensure correct cell division.[50] The checkpoints G1/S and G2/M of the cell cycle are responsible for preventing inappropriate cell cycle progression due to DNA damage or inadequate DNA replication.[51] Cell cycle parameters of HepG-2 cells treated with compounds **7, 19, 26** & **27** were compared with DMSO treated HepG-2 used as control. As shown in Fig. 5, following treatment with **7, 19, 26** & **27** there was a significant decrease

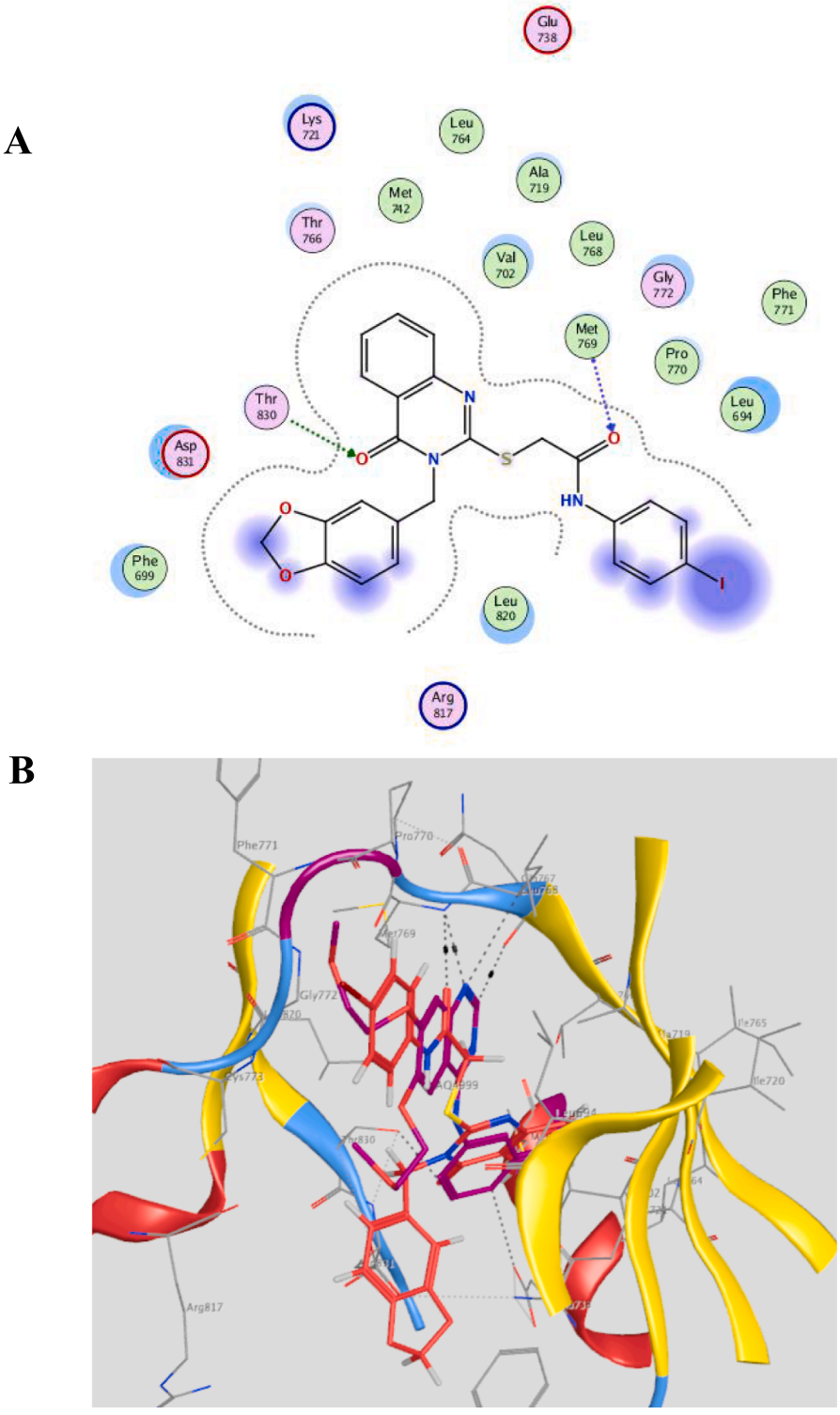

Fig 10. A: 2D interaction pose of compound **27**. **B:** 3 D interaction map of **27** (red), superimposed on the native ligand erlotinib (magenta).

in the fraction of G0-G1 phase (0.039%, 0%, 0.06 % and 0.042% respectively compared to 71.6 % of control) and marked increase in the proportion of cells in G2-M phase (94.2%, 92.9%, 85.8% and 87.8%, respectively compared to 21.7% of control). Also, compounds **7, 19, 26** and **27** have arrested the S phase cells (2.45%, 0.071%, 2.32% and 2.73%, respectively) compared to control with 6.08%. We believe that **19** is superior relative to **7, 26** and **27** as there is almost no S phase arrest with 0.071%, compared to 2.45%, 2.32% and 2.73%, respectively. The p21 gene is a key regulator of the cell cycle that binds to cyclin/CDK complexes and inhibits kinase activation, subsequently blocking cell cycle progression.[50] The observed G2/M arrest followed by induction of apoptosis in treated HepG-2 cells can be explained by up-regulation of p21 expression (Fig. 3**C**). Moreover, cell cycle phases reflect different degrees of radiosensitivity of cells to radiation. The most sensitive phases to radiation are G2 and M phases in contrast to the most radio-resistant S phase point.[51] An interesting finding in our work, G2/M

phase arrest was significantly increased by using flow cytometry upon treatment of HepG-2 cells with **7, 19, 26** & **27** treatments (Fig. 5).

Annexin V assay has revealed that compounds **7, 19, 26** & **27** treatment induced early stage of apoptosis in HepG-2 cells. The Annexin V-FITC plots in Fig. 6 show HepG-2 cell distribution within four different quadrants (Q1, Q2, Q3 and Q4). The data shows a decrease in the percentage of viable cells with a significant increase in the percentage of cells undergoing early apoptosis. A reduction of viable cells was seen in all treated cells in comparison to the untreated cells. The percentage of viable cells has decreased from 94.4 % for untreated cells to 86.1%, 84.5 %, 86.6 %, 92.5 % for **7, 19, 26** & **27,** respectively.

Radiotherapy is a curative treatment for cancer patients mainly through damaging DNA by ionizing radiation.[52,53] Exposing cells to ionizing radiation results in the formation of free radicals by aqueous radiolysis.[54,55] On the other hand, radioresistance of cancer cells is the primary cause of poor prognosis in cancer patients. So, effective radiosensitizers having low toxicity and high selectivity are a must to improve the efficacy of radiotherapy. The quinazoline-based EGFR inhibitor, Gefitinib was identified as an effective radiosensitizer with high selectivity.[56,57] Similarly, in this study we aimed to develop a radiosensitizer with high selectivity by maintaining the EGFR autophosphorylation inhibitory activity. The cytotoxic activities of the most potent compounds **7, 19, 26** and **27** on HepG-2 and MCF-7 cell lines were evaluated after being exposed to a single dose of 8 Gy gamma irradiation. The IC_{50} of the compounds are reported in Table 3; the cytotoxic activities of the compounds have increased after the cells containing the compounds been subjected to irradiation and became in the range of 1.56–4.32 μM for HepG-2 cells and 3.06–5.93 μM for MCF-7 cells. Also, significant downregulation of XIAP and Survivin expression in HepG-2 treated cells relative to untreated control was observed by these compounds as mentioned above thus suggesting their radiosensitizing ability.

To study the binding features of the promising compounds, molecular docking simulations were carried out. Compounds **7, 19, 26** and **27** were selected for evaluating their EGFR inhibitory activity and were docked into the crystal structure of the target kinase in complex with Erlotinib (PDB code: **1M17**).[58] Validation of the docking protocol was initiated by self-docking the native ligand in the binding pocket of EGFR. Self-docking of the native ligand reproduced the key interactions and the binding patterns reported earlier,[59] with an energy score of − 7.20 kcal/mol and RMSD = 1.0352 Å. Energy score and RMSD values are within acceptable limits.[60] The active residues of **1M17** consist mainly of these key amino acids; Met 769, Thr 766, Leu 694, Ala 719, Gln 767, Leu 764, Leu 768, Phe 771, Pro 770, Thr 830, Gly 772, Leu 820 and Asp 831. The 2D and 3D forms of interactions of compounds **7, 19, 26** and **27** were given in Figs.7-10. The quinazolinone scaffold of **7, 19, 26** and **27** is located in an area defined by Thr 766, Met 742, Val 702, Ala 719, Leu 764, Leu 768 and Lys 721 residues. The substituted phenyl group in the acetamide moiety of **19, 26** and **27** were stabilized by the formation of hydrophobic contacts with Leu 694, Leu 820, Pro 770, Gly 772. Compound **7** showed the highest EGFR inhibitory potential with IC_{50}= 207.1 nM, displaying the best binding affinity with the lowest energy score recorded as − 7.45 kcal/mol, and RMSD = 1.1945 Å. Molecular docking interactions of **7** were represented as three hydrogen bonding, two of them are between CO and NH of hydrazide with Met 769 and the third bond between CO of quinazolinone and Thr 830 residue of 2.57, 2.89 and 2.34 Å bond distance, respectively (Fig. 7**A & B**). In the second place came compound **19**, the binding score was computed as − 7.24 kcal/mol with RMSD = 1.3921 Å. It showed two hydrogen bonds between CO of acetamide with Met 769 and CO of quinazolinone with Thr 830 residue with bond distances of 3.02 and 2.93 Å (Fig. 8**A & B**). Compounds **26** and **27** showed the same interactions exerted by **19**. Compound **26** displayed a binding score of − 6.58 kcal/mol and RMSD = 1.5461 Å (Fig. 9) and exerted the same H-bonding as **19** with bond lengths 2.78 & 2.45 Å. While compound **27** showed a binding score of − 6.73 kcal/mol, RMSD = 1.7192 Å and bond lengths of 3.01 & 2.90 Å (Fig. 10).

In summary, a library of quinazolinone derivatives **4-6**, **19**–**27** and quinazolinone-sulfonamide derivatives **7**–**10**, **13, 14, 17** and **18** were synthesized based upon hybridization strategy between the quinazoline ring that constitutes the core of many tyrosine kinase inhibitors and sulfonamide moiety possessing potent anticancer properties. The cytotoxic activities of the newly synthesized compounds were evaluated against HepG-2 and MCF-7 cell lines. The target compounds showed IC_{50} ranging from 2.46 to 36.85 μM for HepG-2 and 3.87 to 88.93 μM for MCF-7 cell lines. The promising derivatives **7, 19, 26** and **27** were selected to be screened as EGFR inhibitors and displayed IC_{50} ranging from 146.9 to 1032.7 nM compared to Erlotinib (IC_{50}= 96.6 nM). Compounds **7, 19, 26** and **27** have decreased the expression level of XIAP and Survivin compared to control, which in turn have increased caspase-mediated apoptosis in HepG-2 cells through significant caspase-3 activation. The increased level of caspase-3 suggests that the tested quinazolinones have targeted XIAP to activate caspases, which in turn have induced apoptosis in HepG-2 cells. Most probably, these four compounds have increased and sensitized HepG-2 to apoptosis through p21 overexpression. Taken together, these results suggest that compounds **7, 19, 26** and **27** treatments have overcome apoptosis resistance by suppressing Survivin, XIAP and overexpressing caspase-3 and p21. The observed G2/M arrest followed by induction of apoptosis in treated HepG-2 cells might be explained by up-regulation of p21 expression. Moreover, flow cytometry analysis of Annexin-V/PI double stain has confirmed compounds **7, 19, 26** and **27** effects on apoptosis through a decrease in the percentage of viable cells with a significant concomitant increase in the percentage of cells undergoing early apoptosis. The radiosensitizing activities of **7, 19, 26** and **27** were studied on HepG-2 and MCF-7 cancer cell lines after being irradiated by a single dose of 8 Gy gamma radiation. The IC_{50} of the promising compounds after irradiation ranges from 1.56 to 4.32 μM for HepG-2 cells and 3.06–5.93 μM for MCF-7 cell lines compared to 2.46–13.17 μM for HepG-2 and 5.86–15.32 μM for MCF-7 before irradiation. The radiosensitizing molecular mechanism of **7, 19, 26** and **27** might explain G2/M phase arrest, p21 overexpression, downregulation of XIAP and Survivin expression in HepG-2 treated cells. The compounds showed an increase in their cytotoxic effect when combined with radiation, confirming their potential radiosensitizing activity. Molecular docking of the promising compounds in the binding site of EGFR showed their ability to reproduce the fundamental interactions explaining the good activity on EGFR. The cytotoxicity, radiosensitization and pro-apoptotic properties of the promising compounds suggest that they could be considered as anticancer and radiosensitizing agents.

Declaration of Competing Interest

The authors declare that they have no known competing financial interests or personal relationships that could have appeared to influence the work reported in this paper.

Acknowledgment

The authors appreciate the staff members of gamma irradiation unit at the National Center for Radiation Research and Technology (NCRRT) for carrying out the irradiation process.

Appendix A. Supplementary data

Supplementary data to this article can be found online at https://doi.org/10.1016/j.bmcl.2021.128308.

References

1 Parsa N. Environmental factors inducing human cancers. *Iran J Public Health.* 2012;41(11):1–9.
2 Padma VV. An overview of targeted cancer therapy. *Biomedicine.* 2015;5(4):19–25.
3 DeVita VT, Chu E. A history of cancer chemotherapy. *Cancer Res.* 2008;68(21):8643–8653.

4 Topcul M, Cetin I. Endpoint of cancer treatment: targeted therapies. *Asian Pac J Cancer Prev*. 2014;15(11):4395–4403.
5 Zhang Q, Kang R, Zeh I, Herbert J, Lotze MT, Tang D. DAMPs and autophagy: cellular adaptation to injury and unscheduled cell death. *Autophagy*. 2013;9(4):451–458.
6 Hanahan D, Weinberg RA. The hallmarks of cancer. *Cell*. 2000;100(1):57–70.
7 Tummers B, Green DR. Caspase-8: regulating life and death. *Immunol Rev*. 2017;277 (1):76–89.
8 Srinivasula SM, Hegde R, Saleh A, et al. A conserved XIAP-interaction motif in caspase-9 and Smac/DIABLO regulates caspase activity and apoptosis. *Nature*. 2001; 410(6824):112–116.
9 Deveraux QL, Reed JC. IAP family proteins—suppressors of apoptosis. *Genes Dev*. 1999;13(3):239–252.
10 Wang K, Wang X, Hou Y, Zhou H, Mai K, He G. Apoptosis of cancer cells is triggered by selective crosslinking and inhibition of receptor tyrosine kinases. *Commun Biol*. 2019;2(1):1–11.
11 Lemmon MA, Schlessinger J. Cell signaling by receptor tyrosine kinases. *Cell*. 2010; 141(7):1117–1134.
12 Dutta PR, Maity A. Cellular responses to EGFR inhibitors and their relevance to cancer therapy. *Cancer Lett*. 2007;254(2):165–177.
13 Ghorab MM, Abdel-Kader MS, Alqahtani AS, Soliman AM. Synthesis of some quinazolinones inspired from the natural alkaloid L-norephedrine as EGFR inhibitors and radiosensitizers. *J Enzyme Inhib Med Chem*. 2021;36(1):218–237.
14 Verbeek BS, Adriaansen-Slot SS, Vroom TM, Beckers T, Rijksen G. Overexpression of EGFR and c-erbB2 causes enhanced cell migration in human breast cancer cells and NIH3T3 fibroblasts. *FEBS Lett*. 1998;425(1):145–150.
15 Bishayee S. Role of conformational alteration in the epidermal growth factor receptor (EGFR) function. *Biochem Pharmacol*. 2000;60(8):1217–1223.
16 Alagarsamy V, Salomon VR, Vanikavitha G, et al. Synthesis, analgesic, anti-inflammatory and antibacterial activities of some novel 2-phenyl-3-substituted quinazolin-4 (3H) ones. *Biol Pharm Bull*. 2002;25(11):1432–1435.
17 Ghorab MM, Alqahtani AS, Soliman AM, Askar AA. Novel N-(Substituted) Thioacetamide Quinazolinone Benzenesulfonamides as Antimicrobial Agents. *Int J Nanomedicine*. 2020;15:3161–3180.
18 Rahman MU, Rathore A, Siddiqui AA, Parveen G, Yar MS. Synthesis and characterization of quinazoline derivatives: search for hybrid molecule as diuretic and antihypertensive agents. *J Enzyme Inhib Med Chem*. 2014;29(5):733–743.
19 Soliman AM, Karam HM, Mekkawy MH, Higgins M, Dinkova-Kostova AT, Ghorab MM. Radiomodulatory effect of a non-electrophilic NQO1 inducer identified in a screen of new 6, 8-diiodoquinolin-4 (3H)-ones carrying a sulfonamide moiety. *Eur J Med Chem*. 2020;112467.
20 Soliman AM, Karam HM, Mekkawy MH, Ghorab MM. Antioxidant activity of novel quinazolinones bearing sulfonamide: Potential radiomodulatory effects on liver tissues via NF-κB/PON1 pathway. *Eur J Med Chem*. 2020;197:112333. https://doi.org/10.1016/j.ejmech.2020.112333.
21 Ghorab MM, Soliman AM, Bua S, Supuran CT. Biological evaluation, radiosensitizing activity and structural insights of novel halogenated quinazoline-sulfonamide conjugates as selective human carbonic anhydrases IX/XII inhibitors. *Bioorg Chem*. 2021;107:104618. https://doi.org/10.1016/j.bioorg.2020.104618.
22 Alsaid MS, Al-Mishari AA, Soliman AM, Ragab FA, Ghorab MM. Discovery of Benzo [g] quinazolin benzenesulfonamide derivatives as dual EGFR/HER2 inhibitors. *Eur J Med Chem*. 2017;141:84–91.
23 Soliman AM, Ghorab MM. Exploration of N-alkyl-2-[(4-oxo-3-(4-sulfamoylphenyl)-3, 4-dihydroquinazolin-2-yl) thio] acetamide derivatives as anticancer and radiosensitizing agents. *Bioorg Chem*. 2019;88:102956. https://doi.org/10.1016/j.bioorg.2019.102956.
24 Bhatia P, Sharma V, Alam O, et al. Novel quinazoline-based EGFR kinase inhibitors: A review focussing on SAR and molecular docking studies (2015–2019). *Eur J Med Chem*. 2020;204:112640. https://doi.org/10.1016/j.ejmech.2020.112640.
25 Shagufta S, Ahmad I. An insight into the therapeutic potential of quinazoline derivatives as anticancer agents. *MedChemComm*. 2017;8(5):871–885.
26 Chegwidden WR, Carter ND. In: *The Carbonic Anhydrases*. Basel: Birkhäuser Basel; 2000:13–28. https://doi.org/10.1007/978-3-0348-8446-4_2.
27 Soliman AM, Ghorab MM, Bua S, Supuran CT. Iodoquinazolinones bearing benzenesulfonamide as human carbonic anhydrase I, II, IX and XII inhibitors: Synthesis, biological evaluation and radiosensitizing activity. *Eur J Med Chem*. 2020; 200:112449. https://doi.org/10.1016/j.ejmech.2020.112449.
28 Ghorab MM, Alsaid MS, Al-Ansary GH, Abdel-Latif GA, Abou El Ella DA. Analogue based drug design, synthesis, molecular docking and anticancer evaluation of novel chromene sulfonamide hybrids as aromatase inhibitors and apoptosis enhancers. *Eur J Med Chem*. 2016;124:946–958.
29 Khanapure SP, Garvey DS, Young DV, et al. Synthesis and structure– activity relationship of novel, highly potent metharyl and methcycloalkyl cyclooxygenase-2 (COX-2) selective inhibitors. *J Med Chem*. 2003;46(25):5484–5504.
30 de Oliveira AN, Bocca CC, Carvalho JE, et al. New substituted 4-arylaminoquinazolines as potent inhibitors of breast tumor cell lines: in vitro and docking experiments. *Eur J Med Chem*. 2010;45(9):4339–4342.
31 Genc Bilgicli H, Taslimi P, Akyuz B, Tuzun B, Gulcin İ. Synthesis, characterization, biological evaluation, and molecular docking studies of some piperonyl-based 4-thiazolidinone derivatives. *Arch Pharm*. 2020;353(1):1900304. https://doi.org/10.1002/ardp.v353.110.1002/ardp.201900304.
32 Pereira GJV, Tavares MT, Azevedo RA, et al. Capsaicin-like analogue induced selective apoptosis in A2058 melanoma cells: Design, synthesis and molecular modeling. *Bioorg Med Chem*. 2019;27(13):2893–2904.
33 Zahedifard M, Lafta Faraj F, Paydar M, et al. Synthesis, characterization and apoptotic activity of quinazolinone Schiff base derivatives toward MCF-7 cells via intrinsic and extrinsic apoptosis pathways. *Sci Rep*. 2015;5(1). https://doi.org/10.1038/srep11544.
34 Wani ZA, Guru SK, Rao AS, et al. A novel quinazolinone chalcone derivative induces mitochondrial dependent apoptosis and inhibits PI3K/Akt/mTOR signaling pathway in human colon cancer HCT-116 cells. *Food Chem Toxicol*. 2016;87:1–11.
35 Nowar RM, A Osman EE, Abou-Seri SM, El Moghazy SM, Abou El Ella DA. Design, synthesis and biological evaluation of some novel quinazolinone derivatives as potent apoptotic inducers. Future. *Med Chem*. 2018;10(10):1191–1205.
36 Yue D, Sun X. Idelalisib promotes Bim-dependent apoptosis through AKT/FoxO3a in hepatocellular carcinoma. *Cell Death Dis*. 2018;9(10):1–11.
37 De AK, Muthiyan R, Mondal S, et al. A natural quinazoline derivative from marine sponge hyrtios erectus induces apoptosis of breast cancer cells via ROS production and intrinsic or extrinsic apoptosis pathways. *Mar Drugs*. 2019;17(12):658. https://doi.org/10.3390/md17120658.
38 Lai K-C, Chia Y-T, Yih L-H, Lu Y-L, Chang S-T, Hong Z-X, et al. Antitumor Effects of the Novel Quinazolinone Holu-12: Induction of Mitotic Arrest and Apoptosis in Human Oral Squamous Cell Carcinoma CAL27 Cells. *Anticancer Res*. 2021;41(1): 259–268.
39 Zhang G-H, Xue W-B, An Y-F, et al. Distinct novel quinazolinone exhibits selective inhibition in MGC-803 cancer cells by dictating mutant p53 function. *Eur J Med Chem*. 2015;95:377–387.
40 Ghorab MM, Alsaid MS, El-Gaby MSA, Safwat NA, Elaasser MM, Soliman AM. Biological evaluation of some new N-(2, 6-dimethoxypyrimidinyl) thioureido benzenesulfonamide derivatives as potential antimicrobial and anticancer agents. *Eur J Med Chem*. 2016;124:299–310.
41 Adams GL, Graybill TL, Sanchez RM, Magaard VW, Burton G, Rivero RA. A convenient 'catch and release'synthesis of fused 2-alkylthio-pyrimidinones mediated by polymer-bound BEMP. *Tetrahedron Lett*. 2003;44(27):5041–5045.
42 Berthelet J, Dubrez L. Regulation of Apoptosis by Inhibitors of Apoptosis (IAPs). *Cells*. 2013;2(1):163–187.
43 Jaiswal PK, Goel A, Mittal R. Survivin: A molecular biomarker in cancer. *Indian J Med Res*. 2015;141(4):389–397.
44 Dizdar L, Tomczak M, Werner T, et al. Survivin and XIAP expression in distinct tumor compartments of surgically resected gastric cancer: XIAP as a prognostic marker in diffuse and mixed type adenocarcinomas. *Oncol Lett.*. 2017 https://doi.org/10.3892/ol10.3892/ol.2017.6999.
45 Abbas T, Dutta A. p21 in cancer: intricate networks and multiple activities. *Nat Rev Cancer*. 2009;9(6):400–414.
46 Hoeferlin LA, Oleinik NV, Krupenko NI, Krupenko SA. Activation of p21-Dependent G1/G2 Arrest in the Absence of DNA Damage as an Antiapoptotic Response to Metabolic Stress. *Genes Cancer*. 2011;2(9):889–899.
47 Ghavami S, Hashemi M, Ande SR, et al. Apoptosis and cancer: mutations within caspase genes. *J Med Genet*. 2009;46(8):497–510.
48 Parrish AB, Freel CD, Kornbluth S. Cellular mechanisms controlling caspase activation and function. *Cold Spring Harb Perspect Biol*. 2013;5(6):a008672.
49 Sanna MG, Correia JdS, Ducrey O, et al. IAP suppression of apoptosis involves distinct mechanisms: the TAK1/JNK1 signaling cascade and caspase inhibition. *Mol Cell Biol*. 2002;22(6):1754–1766.
50 Harper JW, Elledge SJ, Keyomarsi K, et al. Inhibition of cyclin-dependent kinases by p21. *Mol Biol Cell*. 1995;6(4):387–400.
51 Xue J, Zong Y, Li P-D, Wang L-X, Li Y-Q, Niu Y-F. Low-dose hyper-radiosensitivity in human hepatocellular HepG2 cells is associated with Cdc25C-mediated G2/M cell cycle checkpoint control. *Int J Rad Biol*. 2016;92(10):543–547.
52 Hu B, Jin C, Li H-B, et al. The DNA-sensing AIM2 inflammasome controls radiation-induced cell death and tissue injury. *Science*. 2016;354(6313):765–768.
53 Zhang X, Kang Q, Ji Z, et al. Radiosensitization potential of caffeic acid phenethyl ester and the long non-coding RNAs in response to 60Coγ radiation in mouse hepatoma cells. *Radiat Phys Chem*. 2021;181:109326. https://doi.org/10.1016/j.radphyschem.2020.109326.
54 Nair CK, Parida DK, Nomura T. Radioprotectors in radiotherapy. *J Rad Res*. 2001;42 (1):21–37.
55 Liauw SL, Connell PP, Weichselbaum RR. New paradigms and future challenges in radiation oncology: an update of biological targets and technology. *Sci Transl Med*. 2013;5(173):172–173.
56 Zhuang HQ, Sun J, Yuan ZY, Wang J, Zhao LJ, Wang P, et al. Radiosensitizing effects of gefitinib at different administration times in vitro. *Cancer Sci*. 2009;100(8): 1520–1525.
57 Ochs JS. Rationale and clinical basis for combining gefitinib (IRESSA, ZD1839) with radiation therapy for solid tumors. *Int J Rad Oncol Biol Phys*. 2004;58(3):941–949.
58 Stamos J, Sliwkowski MX, Eigenbrot C. Structure of the epidermal growth factor receptor kinase domain alone and in complex with a 4-anilinoquinazoline inhibitor. *J Biol Chem*. 2002;277(48):46265–46272.
59 Ghorab MM, Alsaid MS, Soliman AM. Dual EGFR/HER2 inhibitors and apoptosis inducers: New benzo [g] quinazoline derivatives bearing benzenesulfonamide as anticancer and radiosensitizers. *Bioorg Chem*. 2018;80:611–620.
60 Kramer B, Rarey M, Lengauer T. Evaluation of the FLEXX incremental construction algorithm for protein–ligand docking. *Proteins*. 1999;37(2):228–241.